

Ritonavir Form III: Lightning strikes twice at the same time, 137 miles apart

Stephan D. Parent¹, Pamela A. Smith¹, Dale K. Purcell¹, Daniel T. Smith¹, Susan J. Bogdanowich-Knipp¹, Ami S. Bhavsar², Larry R. Chan², Jordan M. Croom², Haley C. Bauser², Andrew McCalip², Stephen R. Byrn¹, Adrian Radocea^{2*}

1. Improved Pharma LLC, West Lafayette, IN 47906

2. Varda Space Industries, El Segundo, CA 90245

*Corresponding Author: adrian@varda.com

ABSTRACT

Polymorph screening is a crucial step in the characterization and development of pharmaceuticals. The 1998 recall of ritonavir upon the unexpected appearance of the more stable Form II polymorph remains a notorious case of disappearing polymorphs as the presence of Form II inhibited the ability to grow the original Form I. This study presents the characterization of Form III of ritonavir grown from melt/cool crystallization. While Form III has been observed by researchers in 2014 and 2022, this study presents a thorough characterization and novel thermal profile for quicker nucleation and crystallization of the new form. In this work, we expand upon past thermal methods examining the polymorphic landscape of ritonavir to shed light on the crystallization of Form III from the melt.

INTRODUCTION

Since the ritonavir crisis in 1998, when the lifesaving HIV protease inhibitor had to be withdrawn from the market for almost a year due to a sudden and unpredictable appearance of a new less soluble polymorph, ritonavir has been of interest to solid state chemists, crystallographers, and drug development scientists [1-4]. In 2015, a review on disappearing polymorphs highlighted the appearance of ritonavir Form II as perhaps “the most notorious example of disappearing polymorphs” [2]. After the appearance of Form II ritonavir, two new solvates and an anhydrous form were discovered by Morissette et al. [4].

In 2014, Kawakami et al. published their findings after crystallizing ritonavir from its melt. They detected the appearance of a crystalline form after annealing in a 60 °C oven over a period of several days. They concluded that the material was Form IV identified by Morissette et al. [4,5]. However, the x-ray powder diffraction (XPRD) patterns labeled as such do not match the Form IV XRPD pattern in the publication by Morissette et al. [4,5].

Most recently, Yao et al., published a rapid communication, reporting a new anhydrous form, labeled as Form III ritonavir [6]. An overlay of the Form III pattern reported by Yao et al., and the “Form IV” pattern in a 2014 publication by Kawakami et al. suggests that the “Form IV” pattern in the paper was actually a mixture of the new Form III reported by Yao et al., and amorphous material [5,6]. It appears as if Kawakami et al. discovered Form III but did not recognize that it was a new form. To clarify, the label Form III was previously used by Morissette et al. to identify a crystalline solvate [4]. However, this communication follows the Form III naming convention adopted by Yao et al. [6].

Coincidentally, our team was investigating the crystallization of ritonavir from its melt concurrently with Yao et al., and we also identified and characterized Form III. This paper reports that method and several previously unreported properties of Form III ritonavir, demonstrating the value of thermal methods in the discovery of ritonavir polymorphs.

METHODS

Micro-Crystallization (Samples 1a-1e)

Form III was confirmed via Raman microscopy of several samples created during various hot stage optical microscopy (HSOM) experiments. For each experiment, a small portion (~ 0.5 mg) of ritonavir Form II was placed on a scrupulously clean microscope slide. The sample was not covered with a cover glass. The Linkam hot stage system controller was programmed with various temperature ramp routines, as described in Table 1:

Table 1: Thermal Profiles of Ritonavir Micro-Crystallization

| | Sample 1a | Sample 1b | Sample 1c | Sample 1d | Sample 1e |
|---------------|--|--|--|--|--|
| Step1 | Heat 40 °C/min to 127.0 °C hold for 1 min | Heat 40 °C/min to 127.0 °C hold for 1 min | Heat 40 °C/min to 127.0 °C hold for 1 min | Heat 40 °C/min to 127.0 °C hold for 1 min | Heat 40 °C/min to 127.0 °C hold for 2 min |
| Step 2 | Cool 20 °C/min to 70 °C hold for 20 hrs | Cool 20 °C/min to 80 °C hold for 20 hrs | Cool 20 °C/min to 80 °C hold for 20 hrs | Cool 20 °C/min to 80 °C hold for 8 hrs | Cool 20 °C/min to 30 °C hold for 1 hr |

| | | | | | |
|----------------------|--------------------------------------|-------------------------------------|---------------------------------------|---------------------------------------|--|
| Step 3 | Cool 2 °C/min to 30 °C hold for 5 hr | Cool 2°C/min to 30°C hold for 4 hrs | Cool 2 °C/min to 30 °C hold for 5 hrs | Cool 2 °C/min to 30 °C hold for 5 hrs | Heat 2 °C/min to 80 °C hold for 10 hrs |
| Step 4 | N/A | N/A | N/A | N/A | Cool 2 °C/min to 30 °C hold for 10 hrs |
| Raman results | Amorphous, Form III | Form II, Form III, unknown | Form III | Amorphous, Form III | Amorphous, Form III |

In sample 1d, nucleation was evident within 7 minutes and 35 seconds of reaching 80 °C (during step 2), and in sample 1e, nucleation was evident within 17 minutes and 15 seconds of reaching 80 °C (during step 3). Directly upon completion of the hot stage temperature ramp routine, a few crystals of the sample were transferred to either a gold-coated microscope slide or a fused-silica microscope slide and analyzed by Raman microscopy.

Macro-Crystallization (Samples 1f-1g)

A 150.0 mg sample of ritonavir USP lot M-RIT/0804007 Form II was flattened on a glass slide to provide a solid compact of uniform thickness of approximately 1mm x 17mm x 17mm (289 mm³) in size. Using a drying oven, the compact was melted by exposure to 125 to 128 °C for 17 minutes. Temperatures near the vicinity of the sample were measured with a mercury thermometer. The complete melt was confirmed visually. The sample was held at 128 °C for an additional 10 minutes to ensure that no crystalline particles of Form II remained within the melt. The melt was immediately transferred to a second drying oven and placed near a mercury thermometer, also within the oven, measuring 80 °C and retained there for 37 hours. The sample, undisturbed from the glass slide, was removed from the oven and observed with an Olympus SZX9 stereomicroscope under crossed polarizers as a dense mat of birefringent needles. The material was removed from the glass slide and rendered into a powder and analyzed by X-ray powder diffraction, Raman microscopy, and differential scanning calorimetry (DSC). The assigned sample number for this material was 1f and details of the measurement methods are outlined in the Supporting Information.

A 150.0 mg sample of ritonavir USP lot M-RIT/0804007 Form II was flattened on a glass slide to provide a solid compact of uniform thickness of approximately 1mm x 17mm x 17mm (289 mm³) in size. Using a drying oven, the compact was melted by exposure to 125 to 128 °C for 27 minutes. The melt was immediately transferred to a second drying oven and placed near a mercury thermometer, also within the oven, measuring 80 °C, and retained there for 23 hours. The sample, undisturbed from the glass slide, was removed from the oven and observed with an Olympus SZX9 stereomicroscope under crossed polarizers as a dense mat of birefringent needles. The material was removed from the glass slide and rendered into a powder and analyzed by X-ray powder diffraction. The assigned sample number for this material was 1g and measurement specifications are detailed in the Supporting Information.

RESULTS AND DISCUSSION

Figure 1 shows the X-ray diffraction patterns of Form III isolated in samples 1f and 1g (top and bottom, respectively). Figure 2 shows a comparison of XPRD patterns across Morissette et al.'s Form IV, the Kawakami "Form IV" (green and red diffractograms), and Form III characterized in this work. The three combined figures are presented with the x-axes on the same scale, to facilitate comparison. Vertical

dotted lines facilitate comparison of the diffraction peaks for Form III, clearly indicating that the Kawakama patterns do not match Morissette et al.'s Form IV, and in fact match the new Form III. Finally, the XRPD pattern of Form III identified in this work is compared to the XRPD pattern shown by Yao et al. for Form III in Figure 3. Dotted lines are provided to aid comparison, confirming the match.

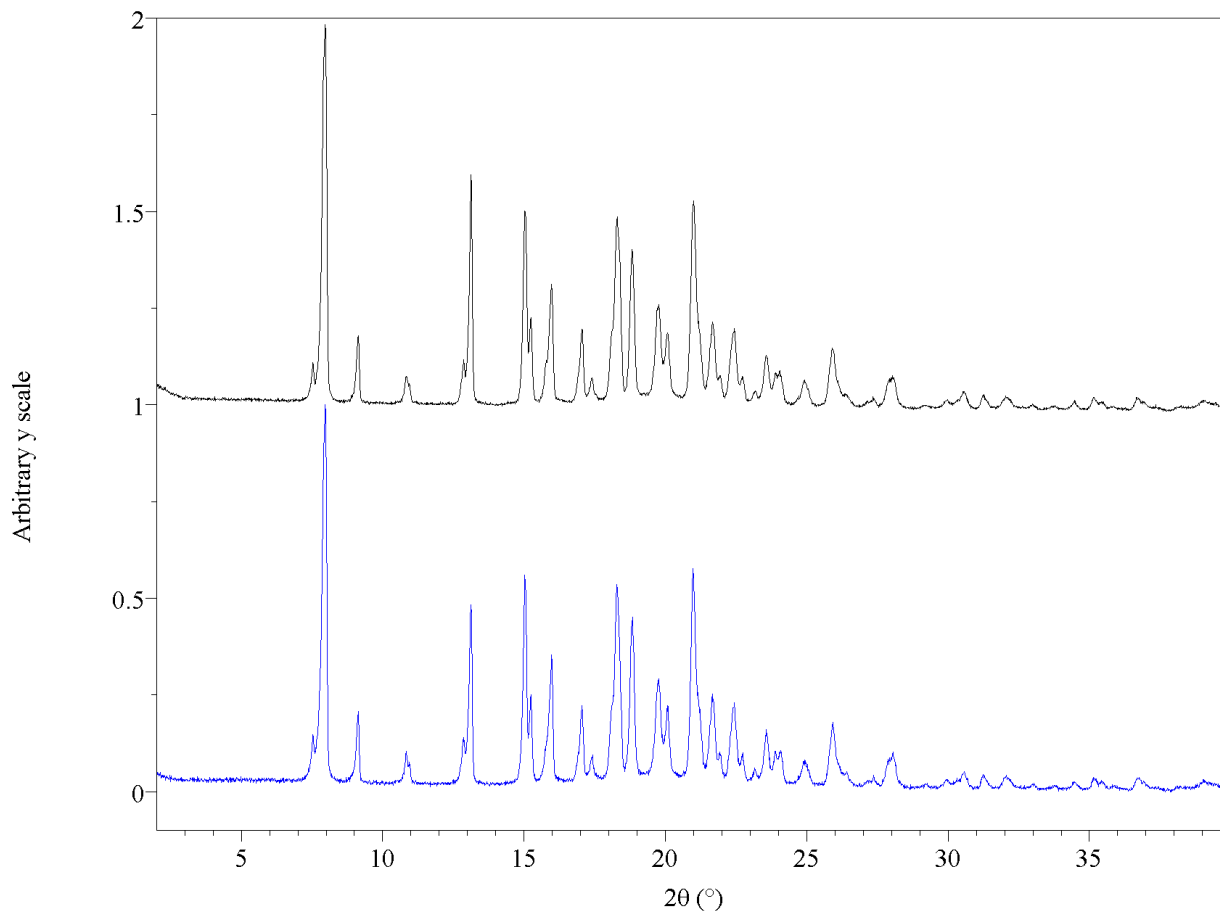
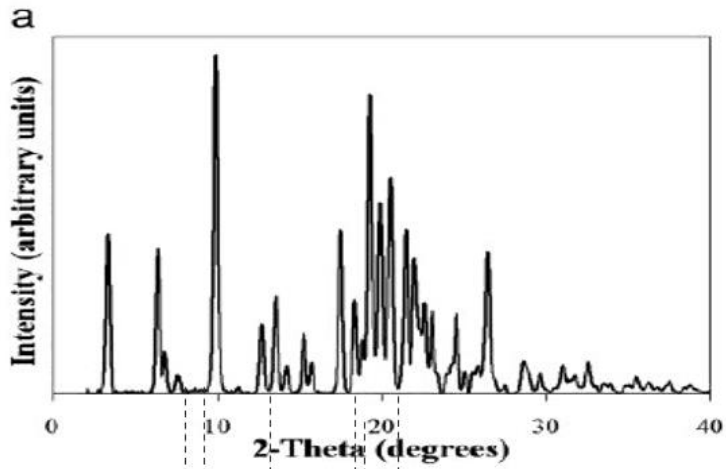
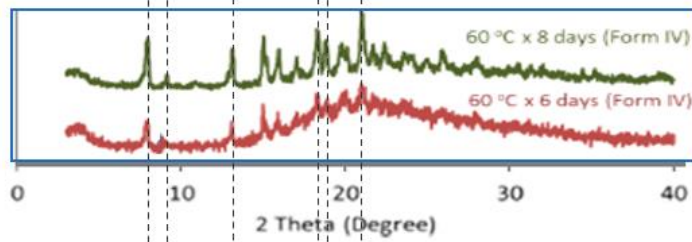


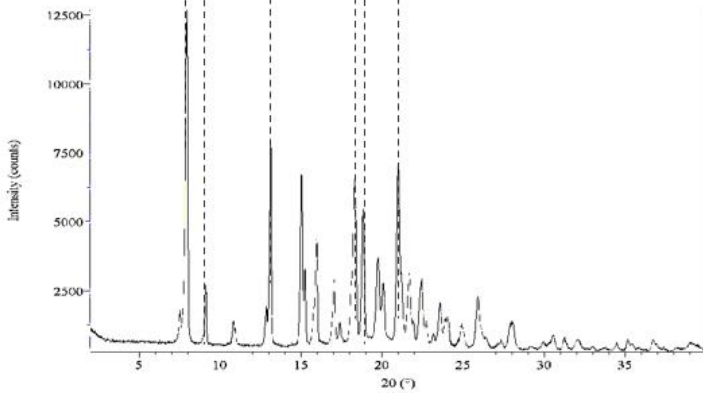
Figure 1 1. X-ray powder patterns for ritonavir Form III obtained at macro scale, samples 1f (top, black) and 1g (bottom, blue).



Morisette et al.
"Form IV"



Kawakami Pattern (a) (8 days)
Kawakami Pattern (b) (6 days)



Presently obtained Form III ritonavir

Figure 2. Comparison of XPRD patterns of Morisette et al.'s Form IV, Kawakami "Form IV", and herein presented Form III [4,5].

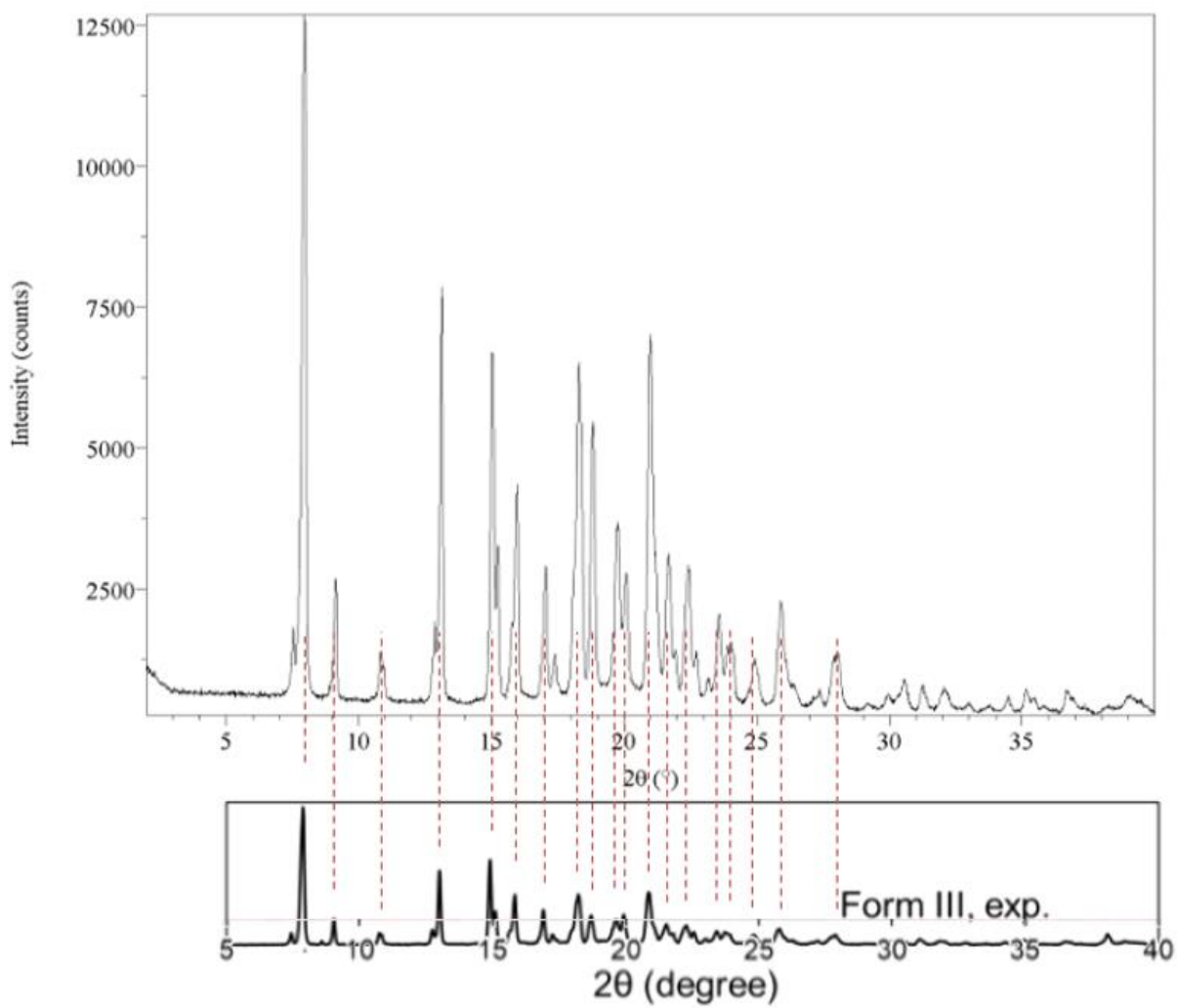


Figure 3. Comparison of XPRD patterns for Form III obtained herein and collected by Yao et al. [6].

The X-ray pattern obtained on Form III sample 1f was analyzed using an indexing method [8]. Indexing is a computational method that searches for a set of crystallographic space group and unit cell parameters that best match the observed Bragg angles in a powder pattern. If successful and all observed Bragg peaks can be attributed to the indexing solution, it is highly likely the XRPD pattern represents a single crystalline phase. The indexing solution can then be used to perform whole-pattern Pawley refinement to accurately determine the unit cell volume and cell parameters and investigate the fit residual for crystalline phase impurities [9]. The successful indexing solution from the pattern is shown in Figure 4 and the cell parameters shown in Table 2. The unit cell parameters are identical, within the expected experimental error, to those published in Yao et al. The differences are attributed to the temperatures at which the powder pattern (at ambient temperature) and the single crystal data (at 150 K) were acquired. Low temperatures are used in single crystal analysis to improve the quality of the structure but can contract the crystal resulting in a change in the unit cell parameters.

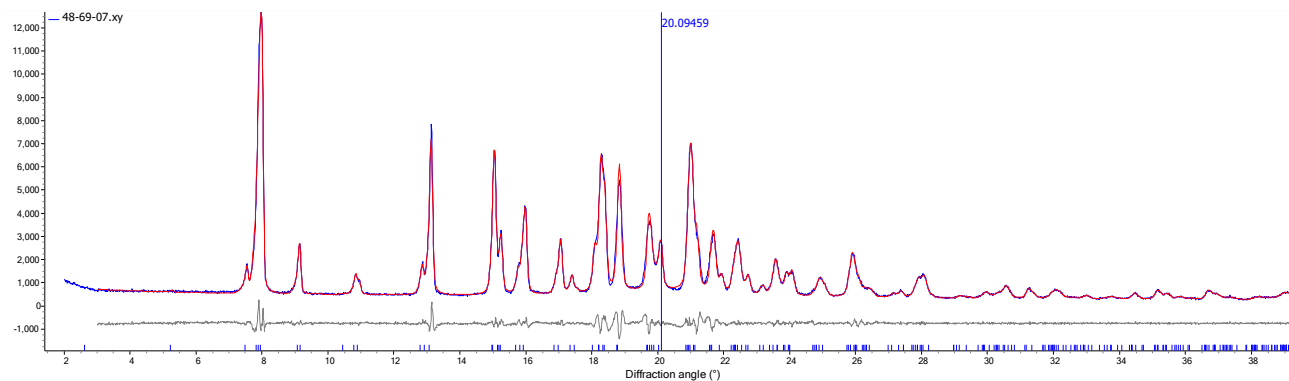


Figure 4. Indexing and Pawley refinement of Form III (sample 1f). Blue: experimental data; Red: fit; Grey: fit residual; Blue notches: allowed peak positions.

Table 2. Pawley Refinement Parameters

| | | | |
|------------------------|--------|--------------------------------|--------|
| Space group | C2 | Cell Volume (\AA^3) | 4031.5 |
| a (\AA) | 23.656 | α ($^\circ$) | 90 |
| b (\AA) | 5.031 | β ($^\circ$) | 90.572 |
| c (\AA) | 33.878 | γ ($^\circ$) | 90 |
| d_{samp} (mm) | -0.154 | | |
| R_{wp} | 6.2% | Density (g/cc) | 1.1878 |

Form III was also characterized by three thermal techniques: DSC, HSOM, and thermogravimetric (TG) analysis. The DSC curve is displayed in Figure 5. The sample has a melt onset temperature of ~ 114 $^\circ\text{C}$, with the endotherm maximum near 118 $^\circ\text{C}$.

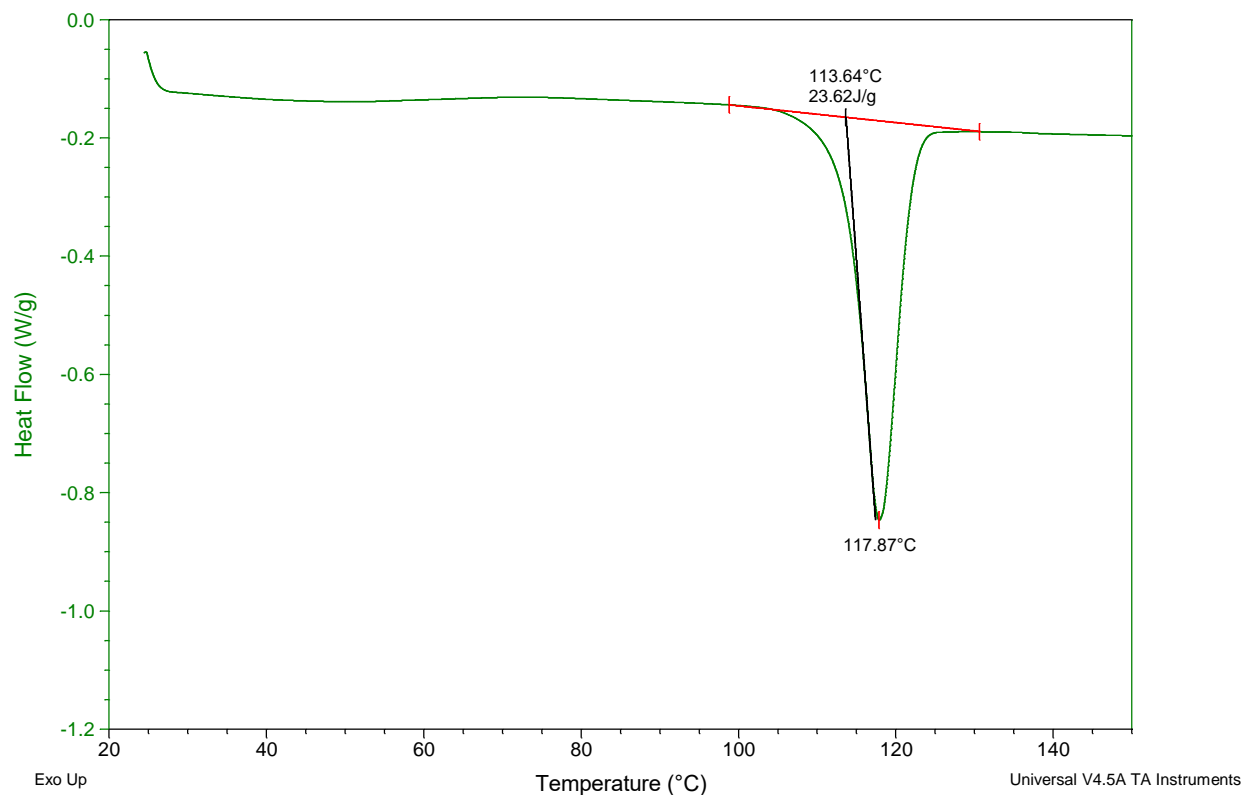


Figure 5. Differential scanning calorimetry thermogram for ritonavir Form III (sample 1f).

Results from the HSOM investigation for the melting point of Form III indicated an onset temperature of 113.7 °C, matching the DSC data. The image of the melt onset is shown in Figure 6, along with images captured at 115.8 °C, 117.0 °C, and 117.9 °C. The sample was completely melted by 117.9 °C and did not recrystallize upon cooling to 26.2 °C. These results conform to the DSC results.

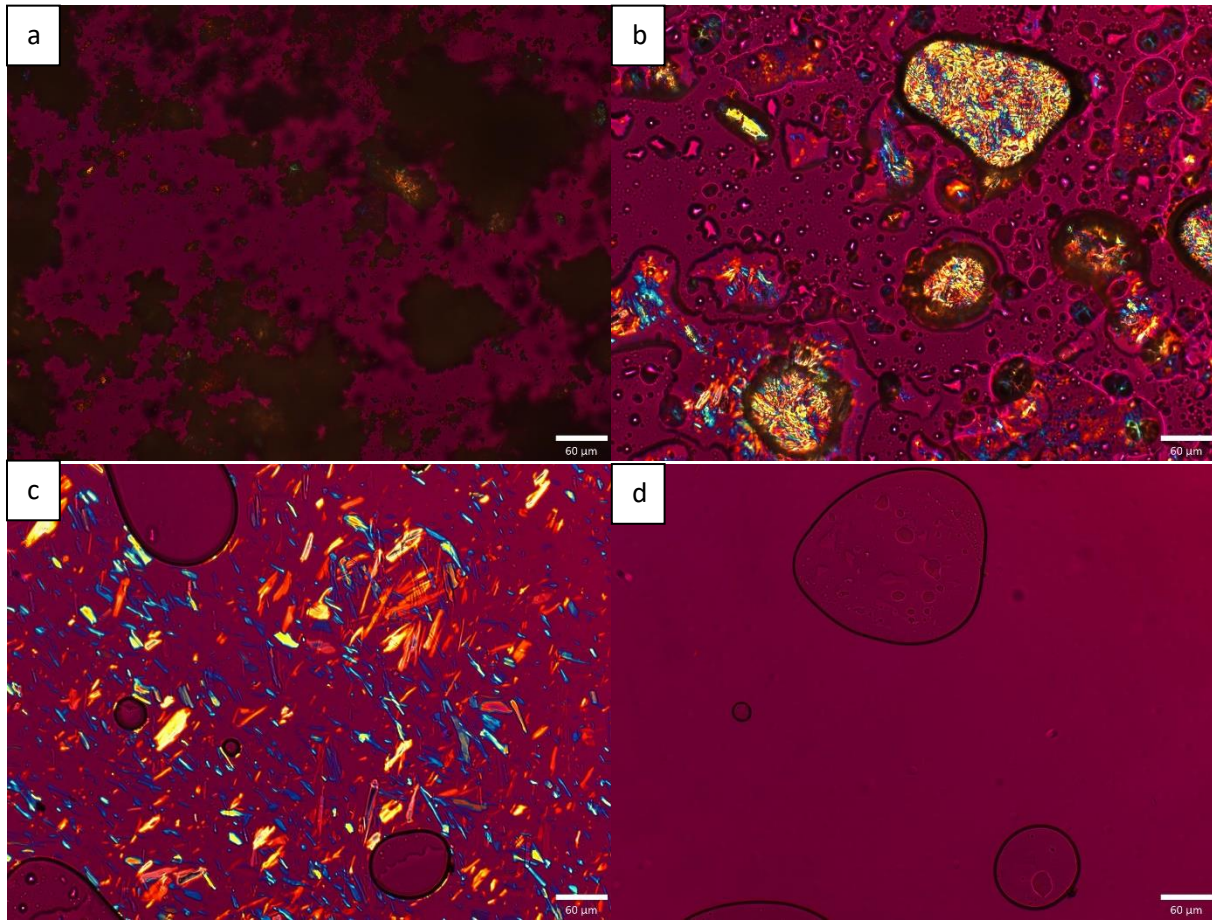


Figure 6. HSOM images for sample 1f: a) Melt onset at 113.7 °C; b) continued melting at 115.8 °C; c) continued melting at 117.0 °C; d) melt complete at 117.9 °C.

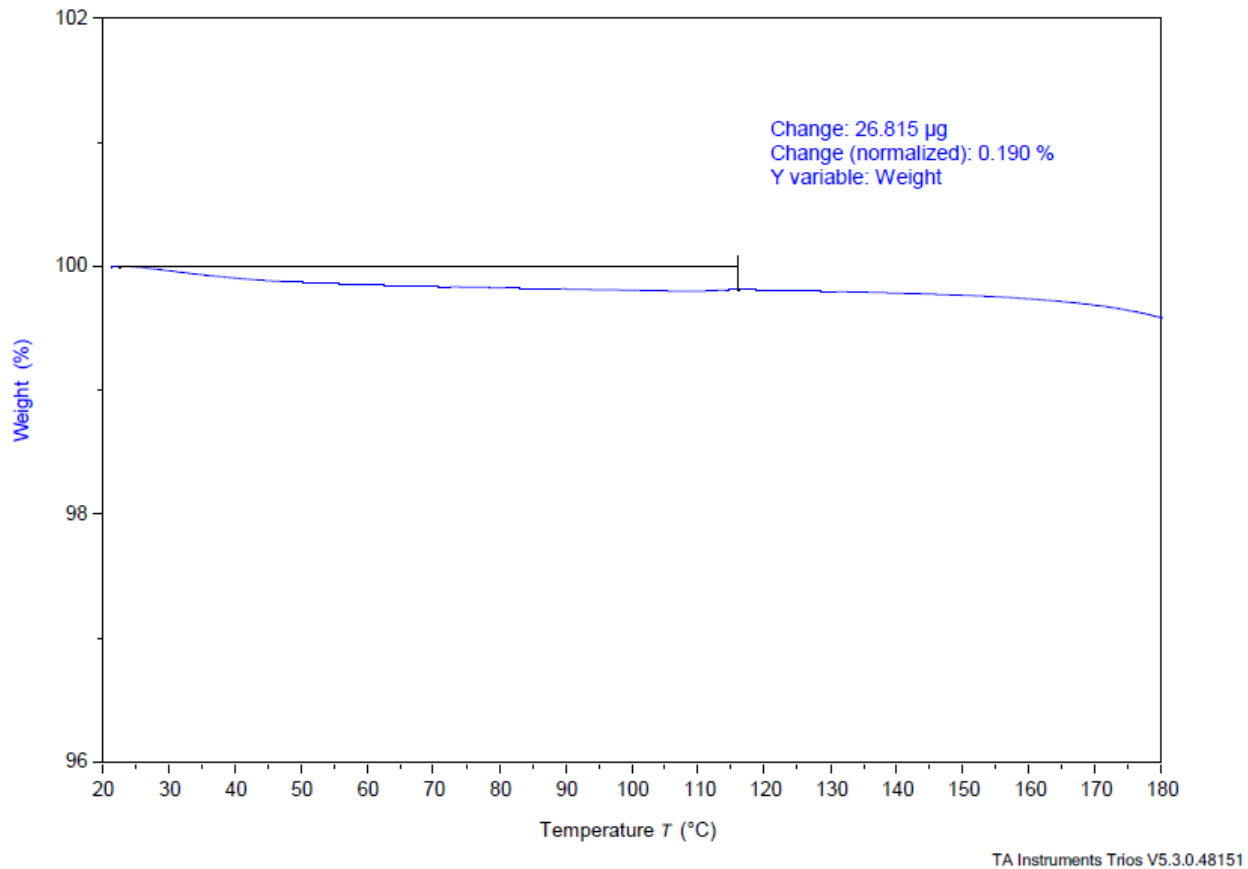


Figure 7. TG thermogram for ritonavir Form III (sample 1f).

TG analysis of Form III did not indicate any appreciable weight loss (Figure 7). The DVS analysis of Form III material is shown in Figure 8. The data indicated that the form was not hygroscopic (very minimal weight gain), which reversed upon the desorption process. No hysteresis was observed.

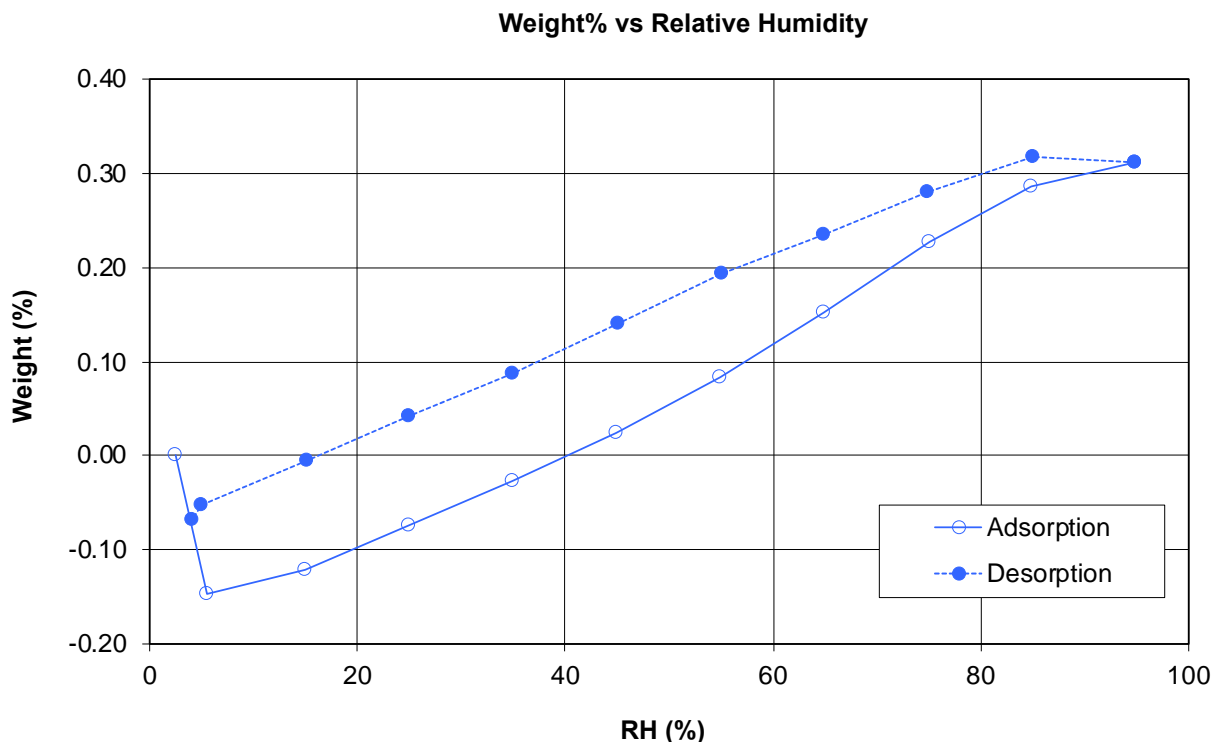


Figure 8. DVS plot for ritonavir Form III (sample 1f).

Several crystals that were created during the HSOM experiments (micro crystallizations) were subsequently analyzed by Raman microscopy. At least five spectra were collected for each sample. In some cases, more than one form was found in each sample. Table 3 below summarizes the Raman findings.

Table 3. Raman microscopy results on HSOM experiments

| Sample | Raman results (number of spectra providing results, out of ten) |
|--------|---|
| 1a | Amorphous (two spectra), Form III (three spectra), mixture Amorphous and Form III (three spectra) |
| 1b | Form II (four spectra), Form III (five spectra), Unknown (one spectrum) |
| 1c | Form III (ten spectra) |
| 1d | Amorphous (three spectra), Form III (one spectrum), mixture Amorphous and Form III (six spectra) |
| 1e | Amorphous (one spectrum), Form III (five spectra), mixture Amorphous and Form III (four spectra) |

Raman spectra were also obtained from the macro crystallization sample (1f). Figure 9 displays the Form III spectrum from the macro experiment along with a representative Form III spectrum from the micro

crystallization experiments (sample 1c). Each spectrum in Figure 9 is an average of 10 separate spectra collected of each sample. The spectra match.

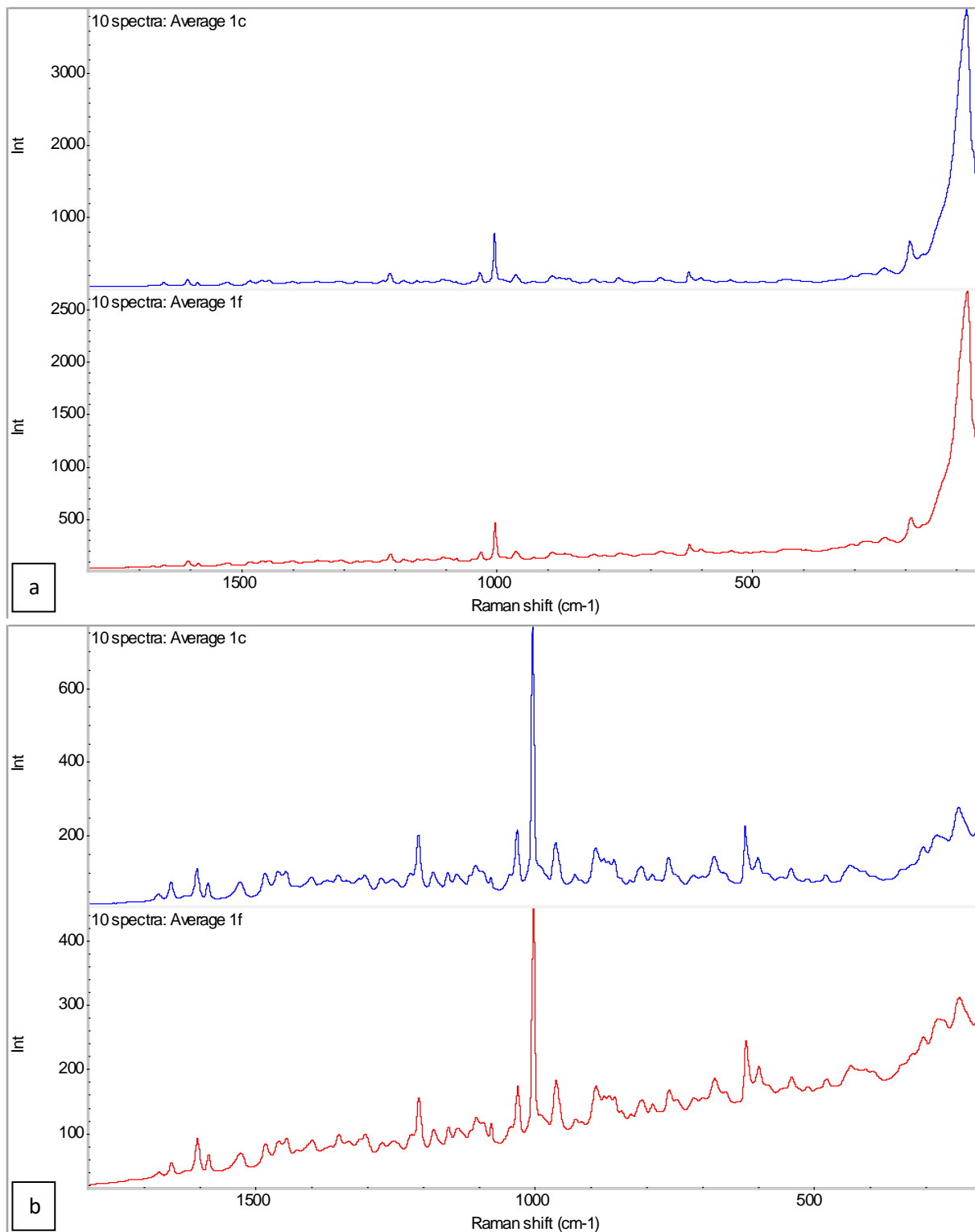


Figure 9. Raman spectra of Form III: a) full spectra range, b) zoomed-in view.

Stability analyses were conducted on Form III (1f) by holding the material sequentially for 15 minutes at 50 °C, 15 minutes at 70 °C, and 15 minutes at 90 °C. The sample was analyzed by Raman microscopy after each temperature exposure. In all cases, the material remained as Form III. Figure 10 compares the short-term thermal stability results to the reference spectra from Figure 9.

Lastly, sample 1c from Table 1 was re-analyzed after storage at ambient conditions for 5 weeks as an additional stability test. The Raman results are presented in Figure 11. Form III (sample 1c) remained unchanged after 5 weeks.

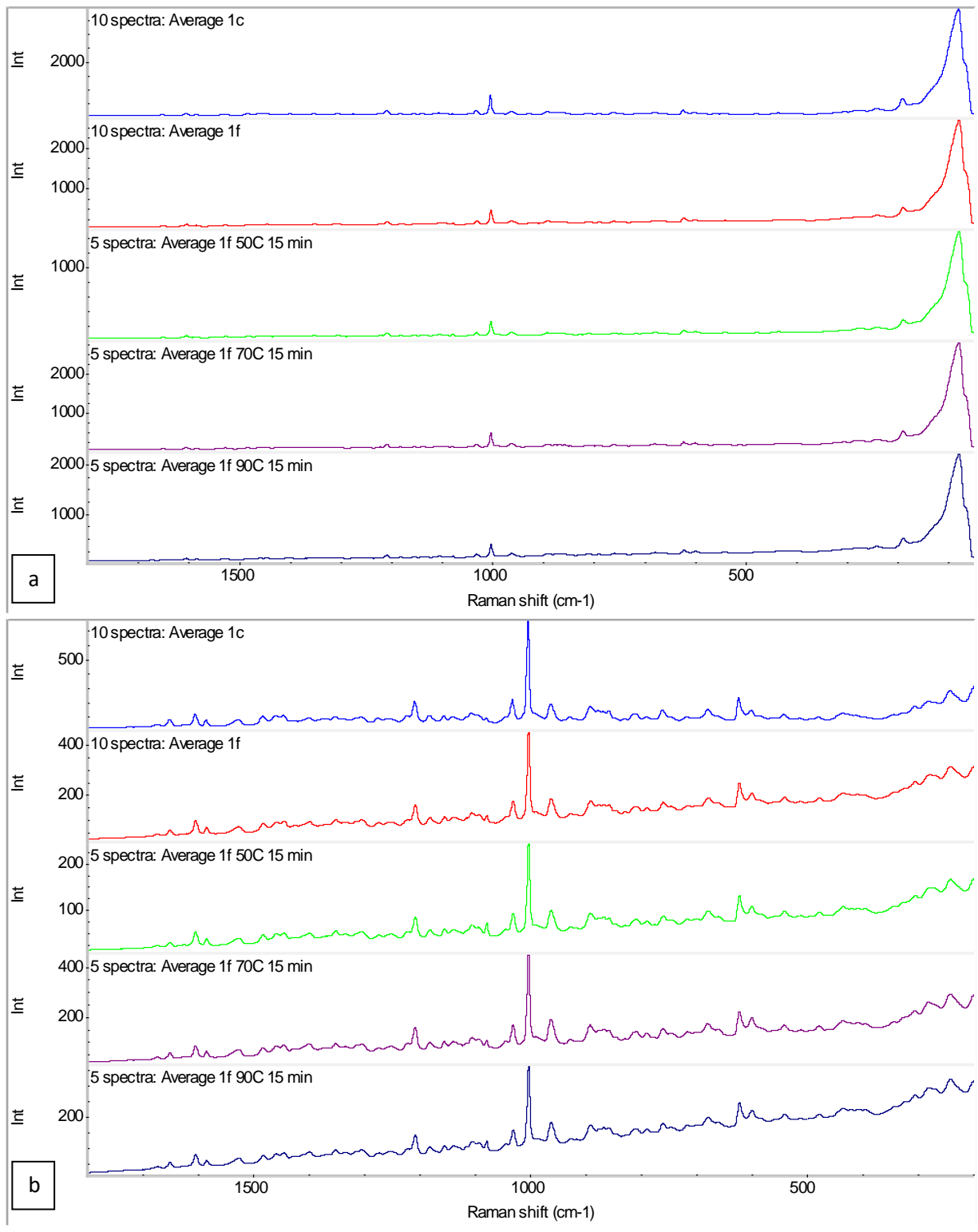


Figure 10. Raman spectra of Form III short-term stability results: a) full spectra range, b) zoomed-in view.

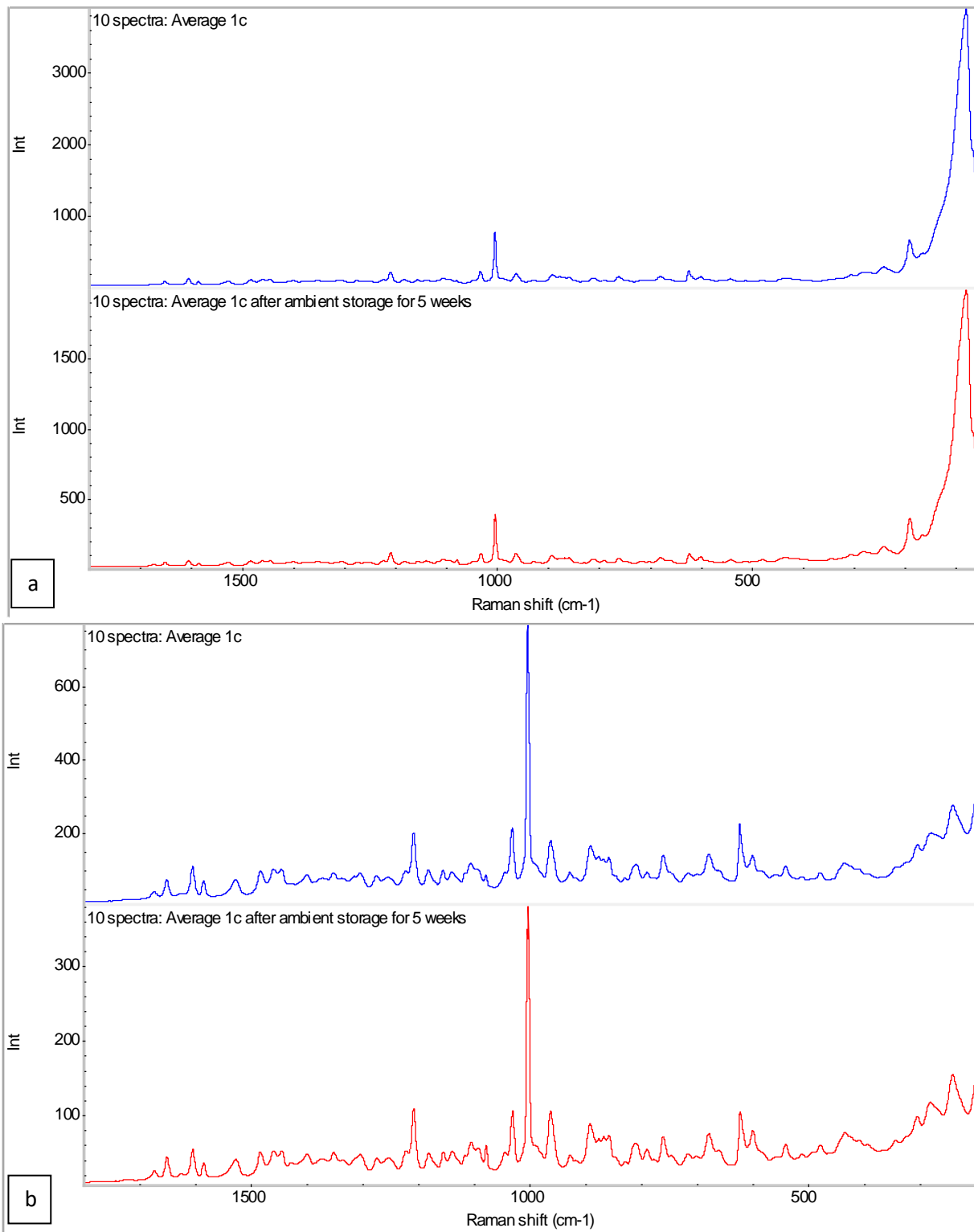


Figure 11. Raman spectra of Form III 5-week stability results: a) full spectra range, b) zoomed-in view.

The optimal nucleation and growth strategy for Form III ritonavir was determined qualitatively from HSOM microcrystallization experiments. The images shown in Figure 12 compare relative concentration of crystals within the supercooled melt when incubated for 5 hours at each of the indicated temperatures. Nucleation at 100 °C did not occur (not shown). The lowest concentration of crystals is evident at both 90 and 70 °C, indicating that nucleation and/or growth is (are) slow at either condition. The highest concentration of well-formed needles is observed when held at 80 °C.

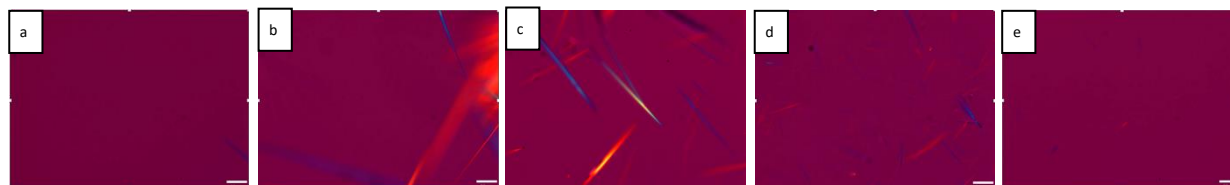


Figure 12. HSOM images of Form III crystals grown from supercooled melts when incubated for 5 hours at: a) 90 °C; b) 85 °C; c) 80 °C; d) 75 °C; and e) 70 °C.

Figure 13 compares the crystal concentration after 5 and 8 hours within the same supercooled melt when held at the ideal temperature, providing a visual representation of the relative crystallization rate achieved. Additional HSOM microcrystallization experiments also determined that (1) first nucleating Form III at a cooler temperature before incubating at a slightly higher temperature did not increase the overall rate of crystallization, while (2) the quench rate from the melt to the incubation temperature does influence the nucleation rate.

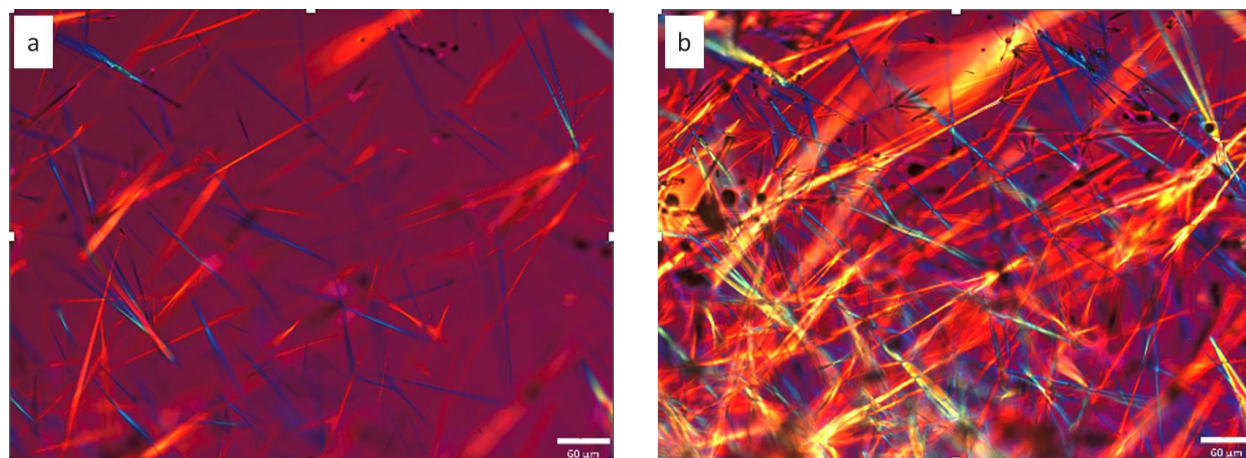


Figure 13. HSOM images of Form III crystals grown at 80 °C from the supercooled melt after a) 5 hours; b) 8 hours.

By applying a general rule of thumb, guidelines based on previously studied systems and the measured glass transition temperature of amorphous ritonavir, Yao et al. assume that the maximum nucleation rate from the melt can only be achieved within a narrow temperature range of 60 – 70 °C [6]. As such, Yao et al. first nucleated Form III at 60 °C for two days, and then continued its growth at 90 °C for an additional two days [6]. However, based on the empirical methodology our team developed, it was determined that these two temperatures are suboptimal for both nucleation and continued growth of

Form III ritonavir from the supercooled melt. Rather, 80 °C was identified as both the ideal nucleation and ideal incubation temperature. Using the optimized conditions illustrated in Figure 14, our team was able to nucleate Form III ritonavir from the melt within a few hours at a micro scale and to nucleate and crystallize completely within 23 hours at a macro scale.

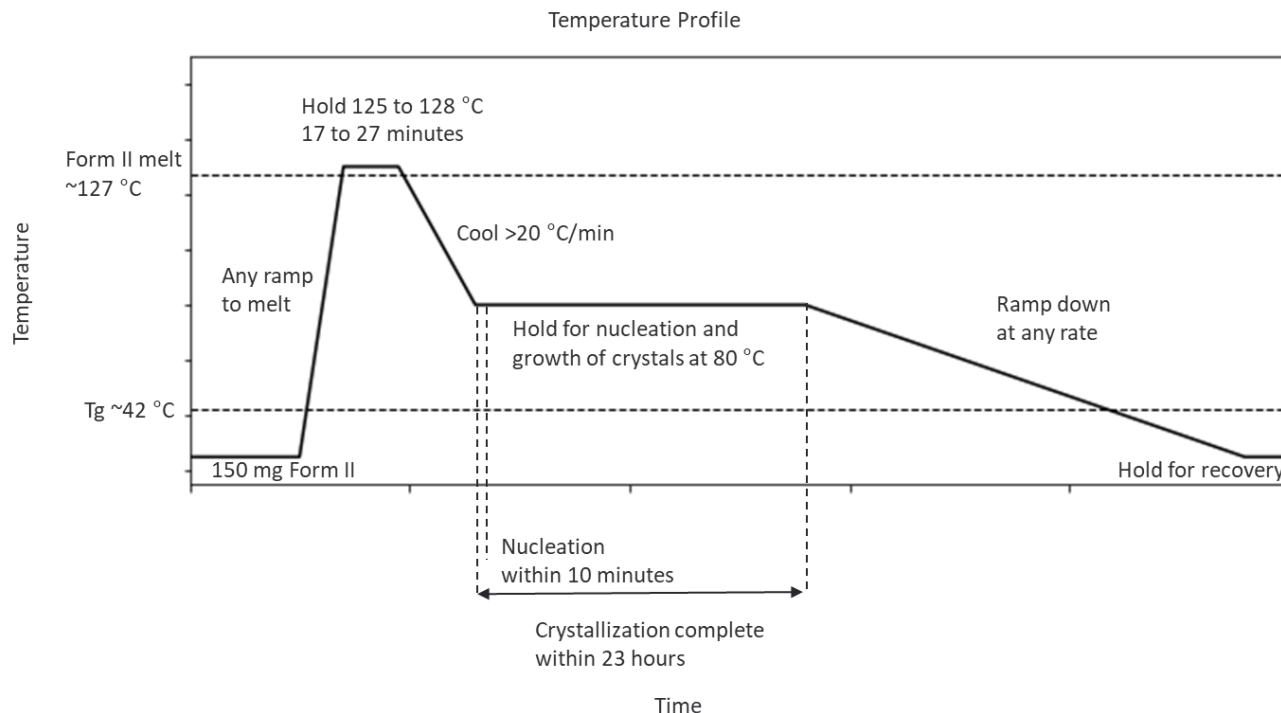


Figure 14. Temperature profile used to provide Form III ritonavir from a supercooled melt within 23 hours.

CONCLUSION

While Form III appears to have been discovered as early as 2014, the recent detailed characterization, analysis, and reproduction of Form III ritonavir adds to the allure of a notorious polymorph. Despite extensive investigation of ritonavir over the past few decades, first a publication in 2014, and now two additional bodies of work have shed light on a new form and its crystallization kinetics. Although it was previously claimed that Form III can only be nucleated between 60-70 °C, and crystallization takes 4 days to complete, this work demonstrates optimized nucleation and growth conditions that reduce the total time to complete crystallization from the melt to less than 23 hours [6]. Lastly, the presented work supports the conclusions of the Yao et al. publication that melt experiments are important for a comprehensive polymorph screening of ritonavir.

REFERENCES

1. Bauer, J., et al., *Ritonavir: an extraordinary example of conformational polymorphism*. *Pharmaceutical research*, 2001. **18**(6): p. 859-866.
2. Bučar, D.K., R.W. Lancaster, and J. Bernstein, *Disappearing polymorphs revisited*. *Angewandte Chemie International Edition*, 2015. **54**(24): p. 6972-6993.

3. Chemburkar, S.R., et al., *Dealing with the impact of ritonavir polymorphs on the late stages of bulk drug process development*. Organic Process Research & Development, 2000. **4**(5): p. 413-417.
4. Morissette, S.L., et al., *Elucidation of crystal form diversity of the HIV protease inhibitor ritonavir by high-throughput crystallization*. Proceedings of the National Academy of Sciences, 2003. **100**(5): p. 2180-2184.
5. Kawakami, K., et al., *Relationship between crystallization tendencies during cooling from melt and isothermal storage: toward a general understanding of physical stability of pharmaceutical glasses*. Molecular Pharmaceutics, 2014. **11**(6): p. 1835-1843.
6. Yao, X., R. Henry, and G. Zhang, , *Ritonavir Form III: A New Polymorph After 24 Years*. 2022.
7. TOPAS 6.0.0.9, 2018, Bruker AXS GmbH, Karlsruhe, Germany
8. Coelho, A.A., "Indexing of powder diffraction patterns by iterative use of singular value decomposition", *J. Appl. Cryst.* **36** (2003) 86-95.
9. Pawley, G.S., "Unit cell refinement from powder diffraction scans", *J. Appl. Cryst.* **14** (1981) 357-361.